ISSN 2277-2685
IJPSL/July. 2023/ Vol-13/Issue-3/43-63
Dr. L. Renuka *et. al* International Journal of Pharmacetical Sciences Letters

Fish Oil Supplementation Mitigates High-Fat Diet-Induced Obesity: Exploring Epigenetic Modulation and Genes Associated with Adipose Tissue Dysfunction in MiceSS

Dr. L. Renuka, A.V.S.Ksheera Bhavani , N. Hemanth kumar , A. Hari Krishna
Assistant professor 1,2,3,4

1. Dr. L. Renuka, Assistant professor, Department of pharmacy Practice, Sri Venkateswara College of pharmacy, Etcherla, Srikakulam. Email: renukalolugu@gmail.com
2. A.V.S.Ksheera Bhavani, Assistant professor, Department of Pharmaceutical Biotechnology, Sri Venkateswara College of Pharmacy, Etcherla, Srikakulam.
3. N. Hemanth kumar, Assistant professor, Department of Pharmacy Practice, Sri Venkateswara College of Pharmacy, Etcherla, Srikakulam.
4. A. Hari Krishna, Assistant professor, Department of Pharmacy Practice, Sri Venkateswara College of Pharmacy, Etcherla, Srikakulam

A. Article Info

Received: 02-03-2023 ***Revised: 05 -04-2023*** ***Accepted: 20-06-2023***

Abstract: To combat obesity caused by a high-fat diet (HFD), this research examined the effects of treating mice with fish oil (FO), specifically FO supplemented with eicosapentaenoic acid (EPA). Understanding how FO affects white adipose tissue (WAT) epigenetic alterations and how adipose-derived stem cells (ASCs) are involved was the primary goal of the study. After 16 weeks on one diet or the other, C57BL/6j mice were split into two groups: control and high-fat diet. Subdividing the HFD group into HFD and HFD + FO (treated with FO) occurred over the final 8 weeks. Isolated, cultured, and treated with leptin ASCs were prepared, while WAT was excised for RNA and protein extraction. Western blotting, real-time polymerase chain reaction, and PCR-array were some of the functional genomics methods used to examine each sample. After a high-fat diet (HFD), mice gained weight, stored more fat, and showed changes in gene expression linked to inflammation and malfunction in the white adipose tissue (WAT). FO supplementation reduced these effects, suggesting a possible preventive function against obesity caused by the HFD. Histone modifications caused by HFD were partly undone by FO therapy, according to H3K27 analysis. In WAT, where leptin levels are high due to obesity, this research dug more into leptin signaling in ASCs, revealing a possible pathway for ASC malfunction. In sum, taking FO supplements effectively reduced HFD-induced obesity, altered molecular and epigenetic pathways, and clarified the involvement of ASCs and leptin signaling in obesity-related WAT dysfunction.

Keywords: obesity; inflammation; H3K27; n-3 PUFA; WAT; leptin

INTRODUCTION:

Complications associated with obesity, such as insulin resistance and cardiovascular illnesses, may arise when the high-fat diet (HFD) model of obesity induction causes inflammation and metabolic dysfunction [1-3]. One important feature of white adipose tissue (WAT) that contributes to obesity-related health problems is the existence of persistent low-grade inflammation, often called "metaflammation" [3–7]. Identifying or guiding the development of therapies targeted at specific inflammatory pathways exacerbated by obesity can provide valuable insights into the underlying mechanisms of these conditions and lead to new approaches for its treatment and management. One

Increasing insulin sensitivity and secretion while decreasing glucose levels are two examples of the natural and synthetic therapies that are gaining favor for controlling obesity caused by high-fat diets (HFDs) [8,9]. According to the same line of thinking, n-3 polyunsaturated fatty acids (PUFA) from fish oil (FO), particularly eicosapentaenoic acid (EPA) and docosahexaenoic acid (DHA), have been shown to improve dyslipidemia, glucose tolerance, insulin sensitivity, and adipose mass in models of obesity caused by high-fat diets (HFD) [10–13]. In our earlier research, we found that obese animals given EPA-enriched FO for eight weeks had a number of positive effects, including decreased body fat and adipose mass, improved adipocyte function, and fewer metabolic and endocrine dysfunctions related to obesity. In addition to its involvement in epigenetically regulating the inflammatory pathway in WAT cells, the fact that FO supplementation reduced the production of pro-inflammatory cytokines raises the possibility that it may help with obesity-related endocrine diseases [14–17]. To accommodate its fast and dynamic capacity to expand or contract, changing lipid storage, WAT must undergo continual remodeling, as is well known, for it to operate properly. Adipocyte differentiation and WAT plasticity are involved in this process, which guarantees that WAT receives oxygen and nutrients and produces the right amount of adipokines [18,19]. Amplified in WAT are adipose tissue-derived mesenchymal stem cells (ASCs), which undergo adipogenesis by epigenetic modifications, most notably the deposition of histone 3 lysine 27 (H3K27) marks [19-22]. The EZH2 enzyme trimethylates H3K27 (H3K27me3), which silences genes (16) and promotes adipogenesis by up-regulating PPARγ and suppressing Runx2. However, these effects may be undone by the H3K27me3 demethylases KDM6A and KDM6B [21,23,24]. On the other hand, CREBBP and EP300 trigger transcription via acetylation (H3K27ac) and have been shown to enhance adipogenesis via their interaction with PPARγ [25]. H3K27 modifiers protect against the harmful effects of hypertrophic obesity by promoting adipogenesis in the right way, which aids in metabolic balance and reduces the risk of chronic inflammation and its complications [21,26]. This, in turn, promotes the formation of healthy adipose tissue. Little is known, however, about how H3K27 marks affect WAT within the setting of chronic inflammatory conditions associated with obesity. The function of H3K27 in controlling fibroblast and monocytic cell inflammatory responses has been well understood in recent years [27,28]. As an example, synergistic induction of CCL2 expression in monocytic cells via H3K27 acetylation was shown in a study including IFN-γ and LPS [27]. Hyperinflammation in fibroblasts is linked to restrictive H3K27 trimethylation, according to another research [28]. These results point to new possible treatment targets.

Regardless, different environmental and physiological stimuli regulate gene expression via the dynamic nature of histone modifications like H3K27ac and H3K27me3. Among the many dynamic chromatin modifications, histone acetylation stands out. A more open chromatin structure that is favorable to gene transcription is produced when lysine residues are added with acetyl groups, as is the case with H3K27ac, and this is substantially affected by the availability of acetyl-CoA [29–31]. Oxaloacetate and acetyl-CoA are produced when citrate and coenzyme A (CoA) are converted by the ATP citrate lyase (ACL) enzyme. The production of acetyl-CoA is an essential first step in many metabolic pathways, and this enzyme is also required for histone acetyltransferases [33], which links metabolism with protein acetylation. There was a significant reduction in acetyl-CoA levels throughout the WAT after four weeks of following an HFD, which is known to inhibit ACL [34–36], as shown by Carrer and colleagues [34]. Further evidence suggests that ACL controls gene regulation and histone acetylation levels [31,37,38]. There is still a lack of knowledge on how obesity affects the regulation of ACL expression in ASCs. It is worth noting that hepatocytes and adipocytes have lower ACL expression when leptin signaling is activated [35]. But if leptin—expressed in obesity-related weight gain tissue (WAT) at high levels—acts paracrinally on adipose stem cells (ASCs) to affect ACL expression—and hence epigenetically

It is yet unknown whether these cells promote differentiation and/or inflammation, which in

turn affects WAT dysfunction. Very little research has investigated whether or if obesity increases the expression of H3K27 modifiers and/or ACL, which are results of persistent low-grade inflammation. The effects of HFD on WAT H3K27ac and H3K27me3 levels, with or without FO supplementation, have also not been well studied. Our HFD-induced obesity mice model showed that the inflammatory route, which is regulated by chemokine and cytokine signaling, was the most significantly impacted signaling system. Notably, FO therapy affected this circuit. It was our intention to learn more about the role of leptin and ACL in this regulation and if it incorporates epigenetic changes to histone 3 lysine 27 (H3K27). We used a mouse obesity model and a battery of functional genomics tests, including real-time polymerase chain reaction (RT-PCR), polymerase array (PCR-array), and Western blot analyses, to try to answer this issue.

1. Results

1.1. Obesity Model Characterization

Obesity parameters were assessed at the end of the 12-week experimental protocol for obesity induction. As expected, there was a decrease in food and caloric intake but an increase in fat intake (~5×, Figure 1A) in mice receiving the HFD. Regarding body mass, a statistical difference between the control group and the groups of animals receiving the HFD became evident from the 3rd week. This difference increased throughout the weeks of the experimental protocol, and by the 12th week of HFD administration, the animals receiving it showed a ~3.5× body mass gain compared to those receiving the CO diet (Fig- ure 1B).

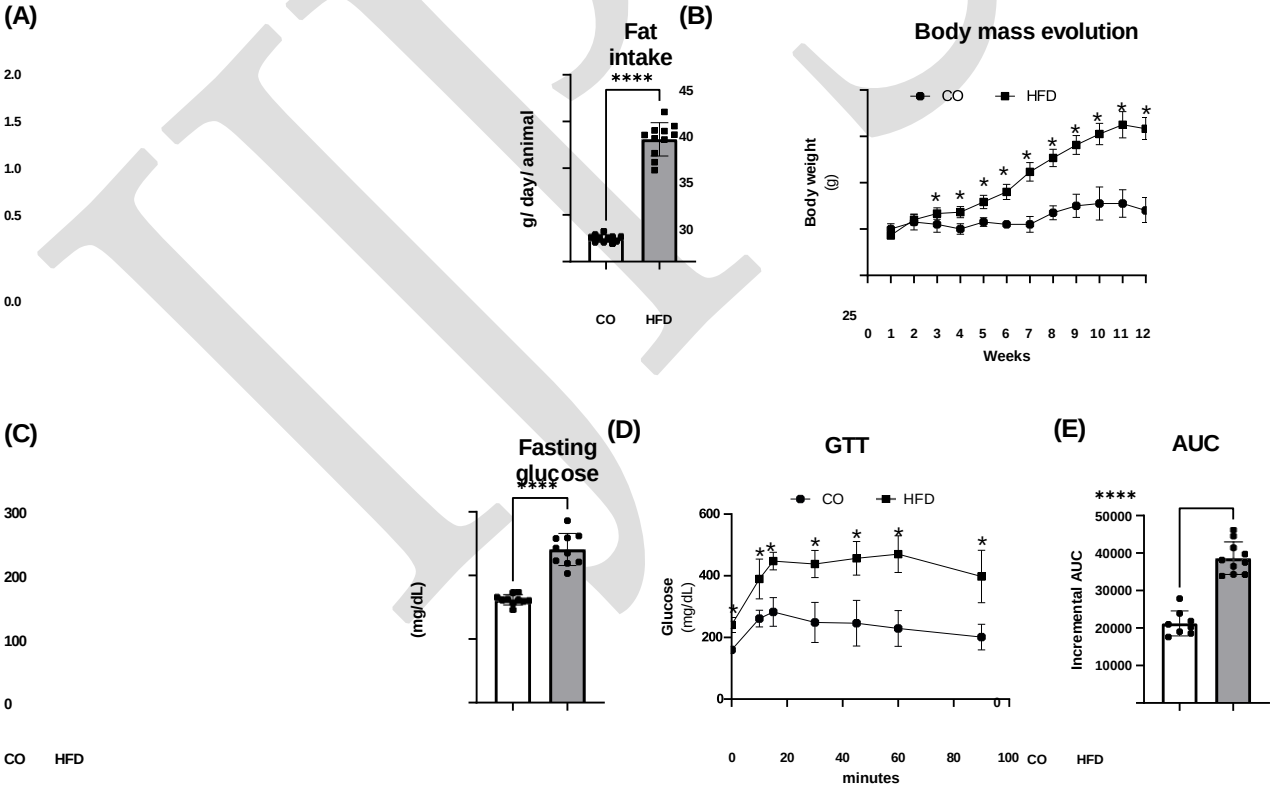

Figure 1. Obesity Model Characterization. (**A**) Caloric (kcal/day/animal), Food and Fat (g/day/animal) intake, (**B**) Body mass evolution, (**C**) Fasting glucose, (**D**) Glucose tolerance test or GTT, and (**E**) Incremental area under the glycemic curve in control (CO) and obese animals induced by a high

fat diet (HFD) for 12 weeks. In (**A**,**B**), the measurements were performed weekly throughout the experimental protocol. In (**C**–**E**), the glycemic curve or glucose concentration versus time was calcu- lated after glucose administration (2 g/Kg b.w.). Data were analyzed using Student's *t*-test, and show mean ± SEM (n = 12). * $p < 0.05$ or **** $p < 0.0001$ versus control.

Figure 1C–E also illustrates values related to fasting blood glucose and the glucose tolerance test (GTT). Compared to the CO diet, mice fed with the HFD showed an approx- imately 50% increase in fasting blood glucose (Figure 1C) and glucose intolerance (Figure 1D), with an expressive (82%) increase in the area under the curve (Figure 1E). Thus, our diet-induced obesity model was characterized, confirming our previous results [15,17,39]. We subsequently supplemented the animals with FO (HFD + FO group) in the last 8 weeks of the 16-week experimental protocol with the HFD.

1.2. WAT depots Extracted from Mice Treated with CO, HFD, and HFD + FO Diets: Depot Mass and Gene Expression by PCR Array

As expected [15,17], mice consuming the HFD presented a significant increase of 50% in body mass when compared to the CO group, and the HFD + FO group was still 40% higher in relation to the CO group, but presented a significant reduction of ~30% ($p < 0.05$) compared to the HFD group (Figure 2A). Moreover, animals in the HFD group exhibited a significant increase in the mass of the visceral epididymal (Epi) fat depot (by ~3×), while treatment with FO completely prevented this increase in fat mass (Figure 2B). However, no significant difference was observed between the HF and HFD + FO groups in the mass of the visceral retroperitoneal (Rp) (Figure 2C) or subcutaneous inguinal (Ing) (Figure 2D) fat depots. The complete metabolic characterization of FO treatment in this model, along with measurements of other tissue weights such as the liver and interscapular brown ad- ipose tissue, has been previously demonstrated and reported in studies conducted by our group [14–17].

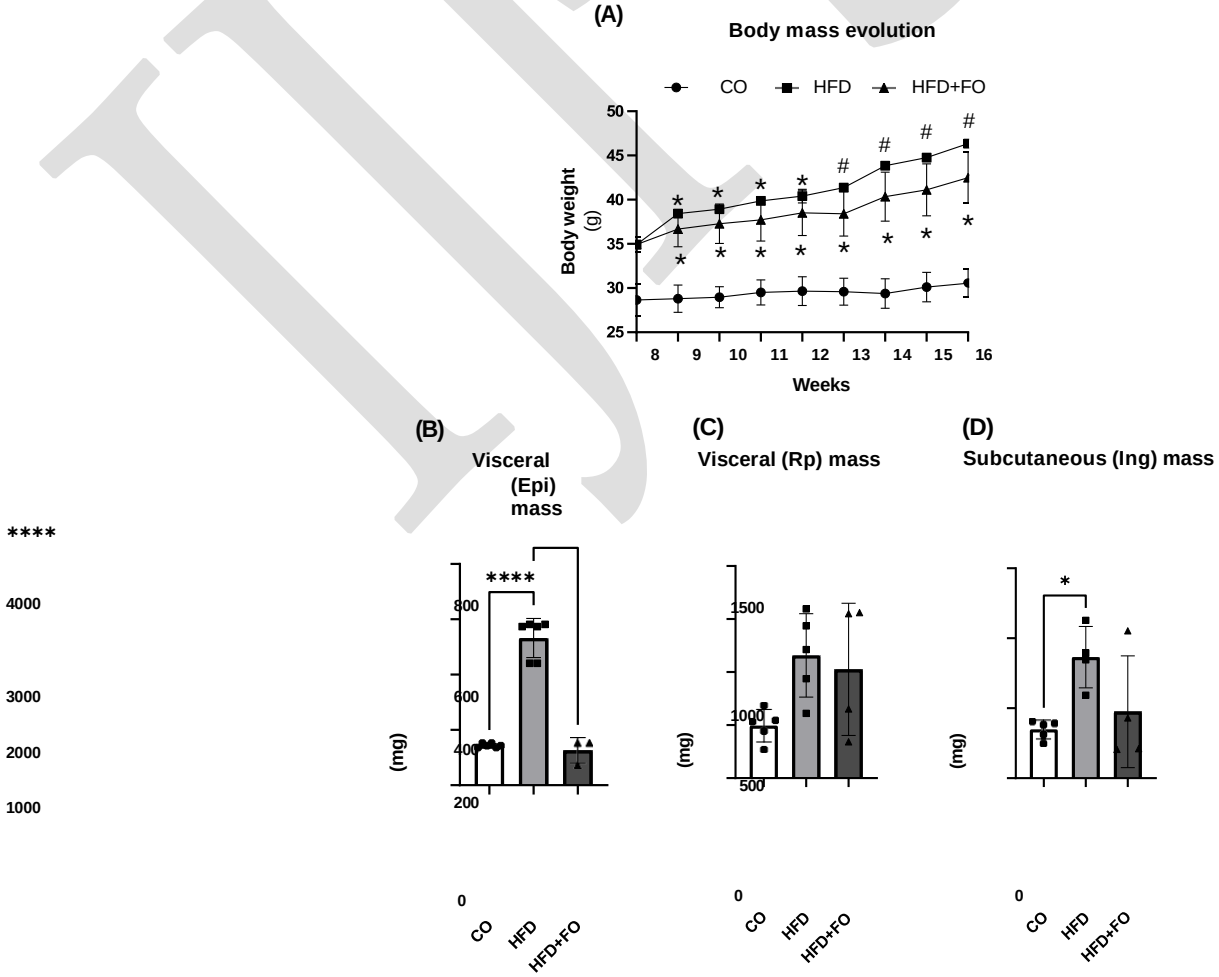

Figure 2. Body mass evolution (**A**), depot mass of visceral epididymal (Epi) (**B**), retroperitoneal (Rp) (**C**), and subcutaneous inguinal (Ing) (**D**) adipose tissues in milligrams (mg), after 16 weeks of ex- perimental diets and fish oil (FO) supplementation. In the initial 8 weeks, the animals were submit- ted to either a control (CO) or high-fat diet (HFD). During the last 8 weeks of the experimental pro- tocol, the diets were continued, and the animals underwent gavage (CO and HFD groups received water, while the HFD + FO group received FO) three times a week. Data were analyzed using one- way Analysis of Variance (ANOVA) followed by Tukey's post-test, and show mean ± SEM (n = 6). * $p < 0.05$ vs. CO, $^{\#}$ $p < 0.05$ vs. CO and HFD + FO, **** $p < 0.0001$.

An analysis of Epi WAT depots (whole tissues) was conducted to explore their gene expression profiles. To do so, we designed a customized panel of 84 essential genes for adipose tissue using a PCR array gene expression assay. Following the validation of reac- tions via array control plates, an in-depth comparative analysis was performed on the tis- sue Ct values to thoroughly examine the gene expression changes induced by the HFD, associated (or not) with FO supplementation. Initially, our emphasis was on scrutinizing genes with differential expression, both up- or down-regulated, attributed to the HFD when compared to the CO diet. These findings, contrasting obese animals with controls, are comprehensively outlined in Table 1.

Table 1. List of genes that were up-regulated and down-regulated, comparing the obesity group to the control group: HFD vs. CO.

Gene Regulation	RefSeq Number	Fold	*p*-Value	Pathway Related
Up-regulated				
Lep	NM_008493	25.48	0.046332	Adipokines
Ncor2	NM_001253904	3.08	ns	Anti-Browning
Dio2	NM_010050	3.98	0.000554	Pro-Browning, fatty acid thermogenesis, and oxidation
Elovl3	NM_007703	2.63	ns	Pro-Browning, fatty acid thermogenesis, and oxidation
Ccl2	NM_011333	5.07	0.009529	Cytokines, growth factors, and signal transduction
Il10	NM_010548	2.08	ns	Cytokines, growth factors, and signal transduction
Tgfb1	NM_011577	3.06	ns	Cytokines, growth factors, and signal transduction
Tnf	NM_013693	10.65	0.009005	Cytokines, growth factors, and signal transduction
Nfkb1	NM_008689	2.52	ns	Cytokines, growth factors, and signal transduction
Cd68	NM_009853	9.16	0.000279	Cytokines, growth factors, and signal transduction
Down-regulated				
Adipoq	NM_009605	−2.82	0.010125	Adipokines
Cfd	NM_013459	−2.54	0.004805	Adipokines
Retn	NM_001204959	−3.30	0.016985	Adipokines
Acaca	NM_133360	−2.55	ns	Lipases and lipogenic enzymes
Scd1	NM_009127	−2.90	0.042774	Lipases and lipogenic enzymes
Lpin1	NM_001130412	−8.55	0.001238	Lipases and lipogenic enzymes
Pck1	NM_011044	−5.98	ns	Lipases and lipogenic enzymes
Fasn	NM_007988	−3.87	ns	Lipases and lipogenic enzymes
Cebpa	NM_007678	−2.45	0.002073	Pro-adipogenesis
Cebpd	NM_007679	−3.64	0.041382	Pro-adipogenesis
Fabp4	NM_024406	−2.01	ns	Pro-adipogenesis
Fgf2	NM_008006	−2.37	ns	Pro-adipogenesis
Fgf10	NM_008002	−2.71	ns	Pro-adipogenesis
Jun	NM_010591	−2.05	ns	Pro-adipogenesis
Sfrp1	NM_013834	−2.98	ns	Pro-adipogenesis

Klf15	NM_023184	−4.62	ns	Pro-adipogenesis
Adrb2	NM_007420	−6.37	0.001464	Anti-adipogenesis
Dlk1	NM_001190703	−2.36	ns	Anti-adipogenesis
Foxo1	NM_019739	−2.26	ns	Anti-adipogenesis
Shh	NM_009170	−18.41	0.000001	Anti-adipogenesis
Wnt1	NM_021279	−4.60	0.001147	Anti-adipogenesis
Wnt3a	NM_009522	−11.21	0.000001	Anti-adipogenesis
Gata2	NM_008090	−2.32	ns	Anti-adipogenesis
Bmp7	NM_007557	−2.06	ns	Pro-Browning, fatty acid thermogenesis, and oxidation
Ppargc1a	NR_027710	−2.40	ns	Pro-Browning, fatty acid thermogenesis, and oxidation
Ppargc1b	NM_133249	−2.29	ns	Pro-Browning, fatty acid thermogenesis, and oxidation
Sirt3	NM_001127351	−2.34	ns	Pro-Browning, fatty acid thermogenesis, and oxidation
Tbx1	NM_011532	−11.21	0.000001	Pro-Browning, fatty acid thermogenesis, and oxidation
Ucp1	NM_009463	−5.67	ns	Pro-Browning, fatty acid thermogenesis, and oxidation
Nr1h3	NM_001177730	−2.28	0.007073	Anti-Browning
Wnt10b	NM_011718	−2.50	ns	Anti-Browning
Lepr	NM_001122899	−2.30	ns	Adipokines receptors
Adipor2	NM_197985	−3.03	ns	Adipokines receptors
Adrb1	NM_007419	−2.73	ns	Adipokines receptors
Ifng	NM_008337	−11.06	0.000001	Cytokines, growth factors, and signal transduction
Il4	NM_021283	−2.20	ns	Cytokines, growth factors, and signal transduction
Il6	NM_031168	−10.93	0.000001	Cytokines, growth factors, and signal transduction
Il13	NM_008355	−11.21	0.000001	Cytokines, growth factors, and signal transduction
Insr	NM_010568	−3.52	ns	Cytokines, growth factors, and signal transduction
Irs1	NM_010570	−4.26	0.043055	Cytokines, growth factors, and signal transduction
Irs2	NM_001081212	−4.61	0.017955	Cytokines, growth factors, and signal transduction
Pik3r1	NM_001024955	−2.33	ns	Cytokines, growth factors, and signal transduction
Irf4	NM_013674	−11.92	0.000978	Cytokines, growth factors, and signal transduction

ns = Not significant. This indicates that, although there was a fold-regulation greater than 2 in the array, the '*p*' value was higher than 0.5, likely due to a large variation resulting from a low number of biological replicates. Nevertheless, these genes may play an important role in the pathways acti- vated by FO in WAT.

Among the various genes modulated, we highlight the up-regulation of the genes *Lep* (+25.48×), *Ncor2* (+3.08×), *Ccl2* (+5.07×), *Tnf* (+10.65×), *Nfkb1* (+2.52×), and *Cd68* (9.16×), triggered by the HFD when compared to the CO group (Table 1). With the exception of *Ncor2* (anti-adipogenic factor), all these genes encode cytokines (*leptin*, *Tnfa*) and macrophage chemotactic factors (*Ccl2*/*Mcp-1*) or markers of macrophages (*Cd68*) and inflammation pathways (NFkB). There was also an increase in *Dio2* (+3.98×) and *Elovl3* (+2.63×), indicating an increase in diet-induced thermogenesis.

We also observed that the HFD suppressed the expression of numerous genes, including those encoding adipokines (adiponectin and resistin), enzymes involved in lipid biosynthesis (*Acc1*, *Scd-1*, *Lipin1*, *Pck1*, and *Fas*), factors related to adipogenesis (*Cebpa*, *Ce- bpd*, *Fabp4*/*Ap2*, *Fgf-2*, *Fgf-10*, *AP-1*/*C-Jun*, *Sfrp1*, *Klf15*, *Adrb2*, *Dlk1*/*Pref-1*, *Foxo-1*, *Shh*, *Wnt1*, *Wnt3a*, *Gata2*), proteins associated with browning, thermogenesis,

(*Bmp7*, *Pgc1-a*, *Pgc1-b*, *Sirt3*, *Tbx1*, *Ucp1*, *Nr1h3*, *Wnt10b*), adipocyte receptors (*Lepr*, *Adipor2*, *Adrb1*), pro- and anti-inflammatory cytokines (*Ifn-γ*, *Il1-β*, *Il-6*, *Il-13*), and insulin sig- naling pathway proteins (*Insr*, *Irs-1*, *Irs-2*, *Pik3r1*).

The data concerning both up-regulated and down-regulated genes in the samples from the HFD and HFD+FO groups are visualized in a heatmap (clustergram, Figure 3). It was evident that the treatment of obese mice with FO altered the extensive list of genes negatively affected by the HFD, inducing an increase in the expression of most of those genes (and others). These encompass genes encoding adipokines (adiponectin, leptin, and resistin), lipolytic and lipogenic enzymes (*Scd-1*, *Lpl*, *Lipin1*, *Pck1*), pro-adipogenic factors (*Cebpa*, *Pparg*, *Srebp-1*, *Fabp4*/*aP2*, *Sfrp1*, *Glut4*), proteins involved in browning and ther- mogenesis, mitochondrial biogenesis, and fatty acid oxidation (Dio-2, Elovl3, Foxc2, Ppar- α, Pgc1-α, Tbx1, Tfam, Ucp-1), pro- and anti-inflammatory cytokines (Mcp-1, Cxcl10, Il1- B, Il-4, Il-6, Il-13, Resistin), and signaling transduction factors (Irs-1, Nf-kb).

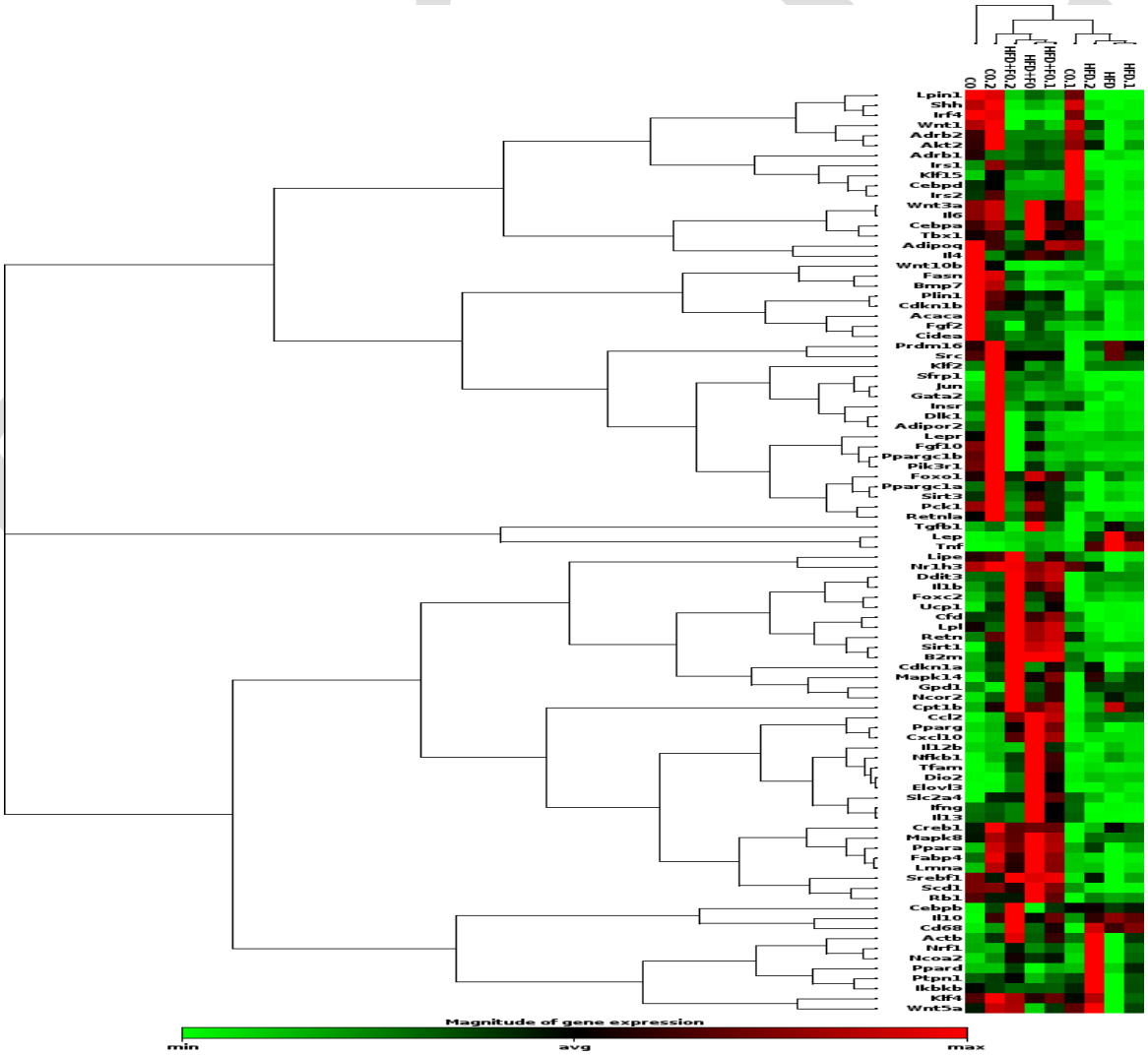

Figure 3. Heatmap of gene expression in Epi WAT from mice subjected to 16 weeks of experimental diets and fish oil supplementation. Control diet (CO), high-fat diet (HFD), and high-fat diet plus fish oil (HFD + FO). The gene expression level is indicated using a color scale, where red indicates higher expression and green indicates lower expression.

1.3. Expression of H3K27 Modifiers, H3k27ac, H3k27met3, and Acly/ACL in the visceral Epi WAT from Mice

Regarding possible alterations in epigenetic marks, we initially assessed the expres- sion of genes encoding enzymes responsible for acetylation (*Ep300* and *Crebbp*), as well as methylation (*Ezh2*) and demethylation (*Kdm6a* and *Kdm6b*) of H3K27 in visceral Epi WAT of control mice, obese mice (HFD), and obese mice treated with FO (HFD + FO). There was no statistically significant difference observed in the transcript levels of *Ezh2* (Figure 4B). However, the genes encoding the acetylases *Crebbp* (Figure 4C) and *Ep300* (Figure 4D), as well as the demethylase *Kdm6b* (Figure 4F), demonstrated a notable increase in expression within the HFD group compared to the control. This effect was completely reversed by FO treatment for *Crebbp* and *Ep300*, while partially reversed for *Kdm6b*. Additionally, no difference was noted between the groups in the expression of the gene encoding the en- zyme *Kdm6a* (Figure 4E).

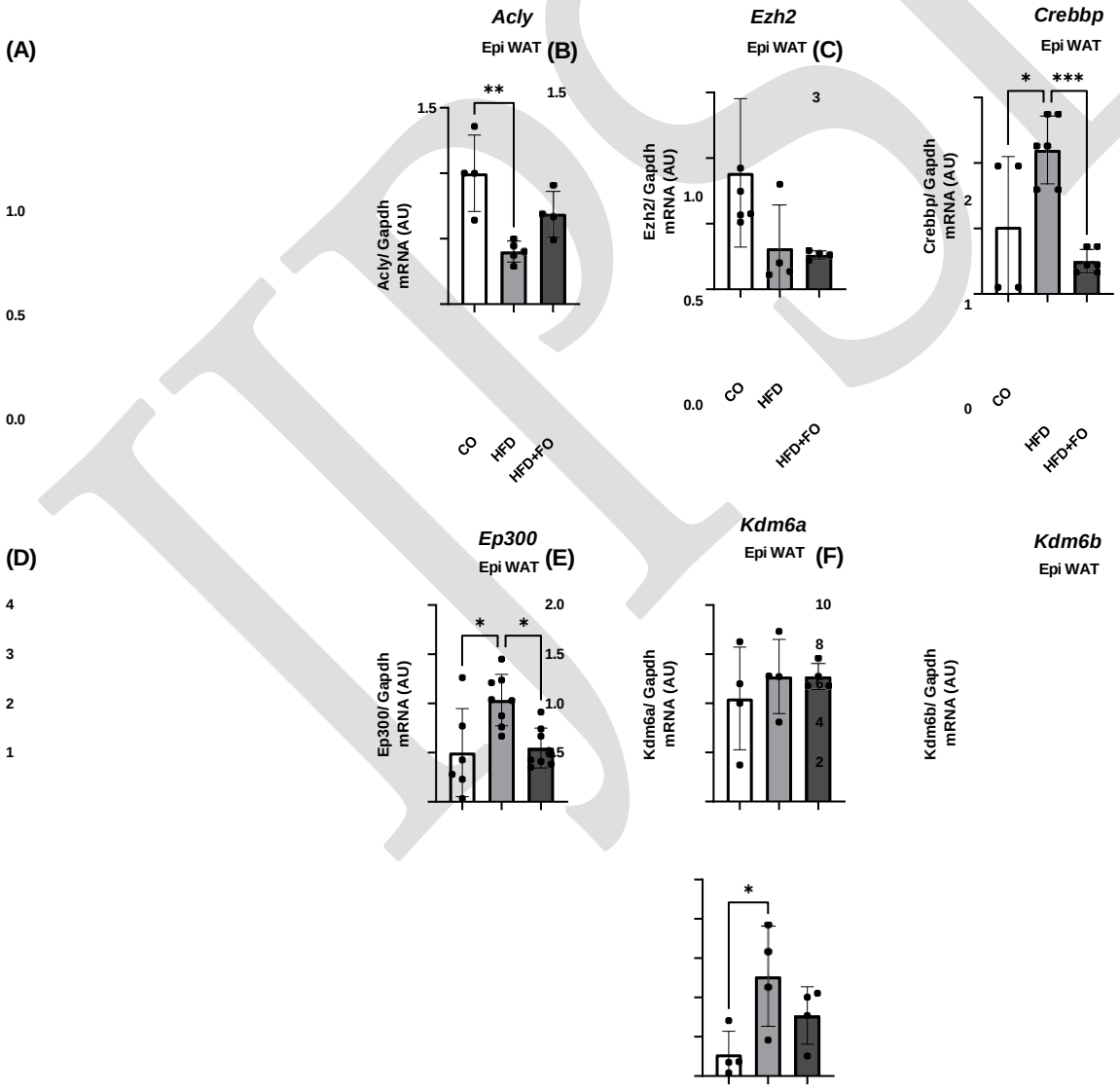

Figure 4. Gene expression of *Acly* (**A**) and genes encoding histone modifiers *Ezh2* (**B**), *Crebbp* (**C**), *Ep300* (**D**), *Kdm6a* (**E**), and *Kdm6b* (**F**), in the visceral Epi WAT from animals that received control diet (CO), high-fat diet (HFD), or HFD and fish oil (HFD + FO). Target genes were normalized by the constitutive *Gapdh.* Data were analyzed using one-way ANOVA followed by Tukey's post-test, and show mean ± SEM (n = 4–6). * $p < 0.05$ or ** $p < 0.003$ or *** $p < 0.001$.

We next investigated the expression of the *Acly* (gene) and ACL (protein), as well as histone-modifying proteins. Consistent with the decreased *Acly* expression (Figure 4A), we observed a reduction in ACL expression in the visceral Epi WAT of obese animals (Fig- ure 5A). Corroborating these findings, we detected a decrease in the expression of H3K27ac in the group of animals with obesity induced by the HFD (Figure 5B), and once again, FO was able to completely prevent this effect. Finally, a significant decrease in the expression of the H3K27me3 protein was also observed (Figure 5C), an effect partially prevented by FO.

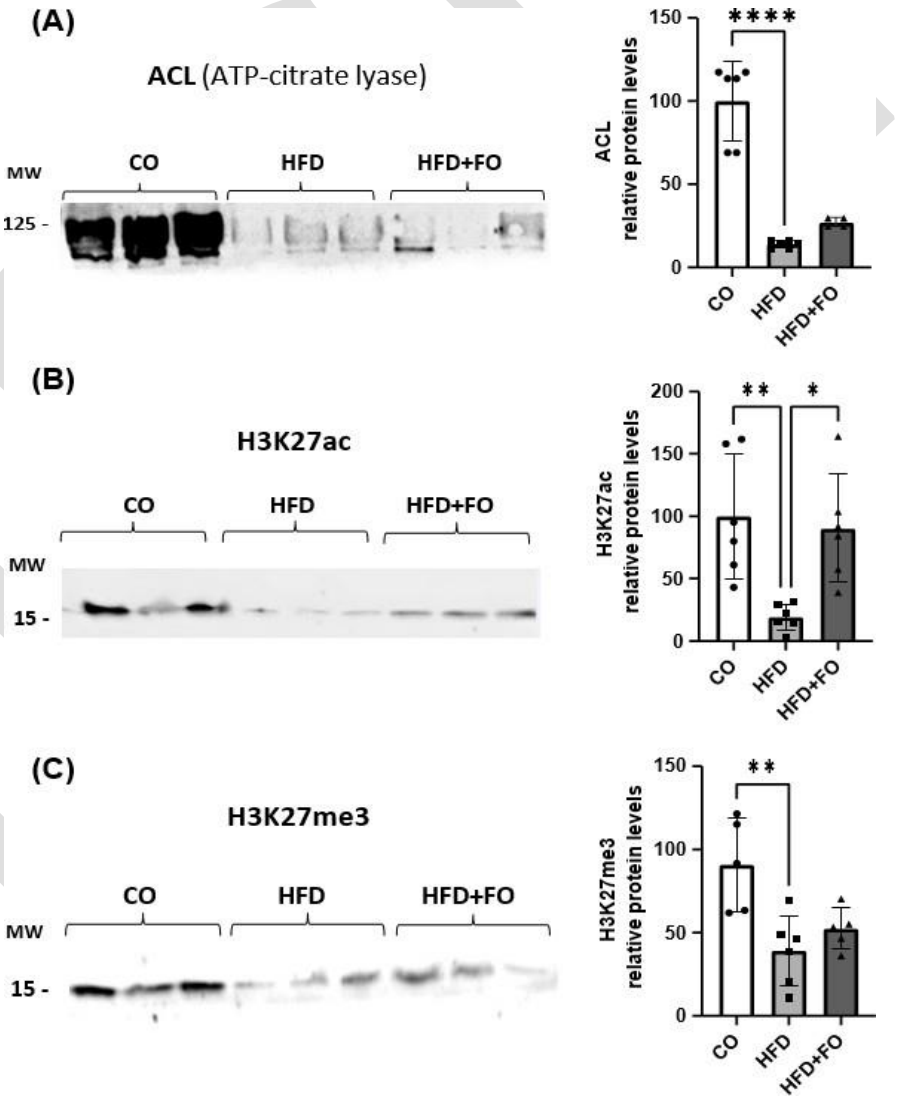

Figure 5. Graphical representation of the protein content of ACL (**A**), H3K27ac (**B**), and H3K27me3 (**C**), in visceral Epi WAT from animals that received a control diet (CO), a high-fat diet (HFD), or an HFD diet and fish oil (HFD + FO). Data were analyzed using one-way ANOVA followed by Tukey's post-test. Values were expressed as mean ± SEM, in relation to the control and corrected by the expression of the constitutive beta-actin and total protein by Ponceau. A representative image of protein expression levels from 2 independent experiments is shown above each graph (n = 3 ani- mals) quantified by ImageJ (Software v1.5.4e). * $p < 0.05$ or ** $p < 0.001$ or **** $p < 0.0001$.

1.4. Gene Expression of Acly and Leptin Receptors in ASCs from Mice

In Figure 6, we validated the expression of *Lepr1* and *Lepr2* receptor isoforms in ASCs. We observed that ASCs extracted from the visceral WAT showed no difference in receptor isoform expression between the CO and HFD animal groups (Figure 6A,B). Moreover, *Lepr3* isoform was not expressed in these cells. When we treated these mice ASCs with leptin (in vitro for 24 h) and examined the expression of LEP protein receptor (long iso- form, Ob-Rb, responsible for total signal transduction), we found that ASCs fully ex- pressed these receptors, whose expression remained unchanged when the ASCs were ex- posed to leptin (Figure 6C). Finally, we evaluated the expression of the *Acly* gene in these ASCs treated in vitro with leptin. Interestingly, we observed a reduction in Acly expres- sion in the HFD mice group. This finding suggests that, in a leptin-rich medium, ASCs exhibit a decrease in *Acly* expression (Figure 6D).

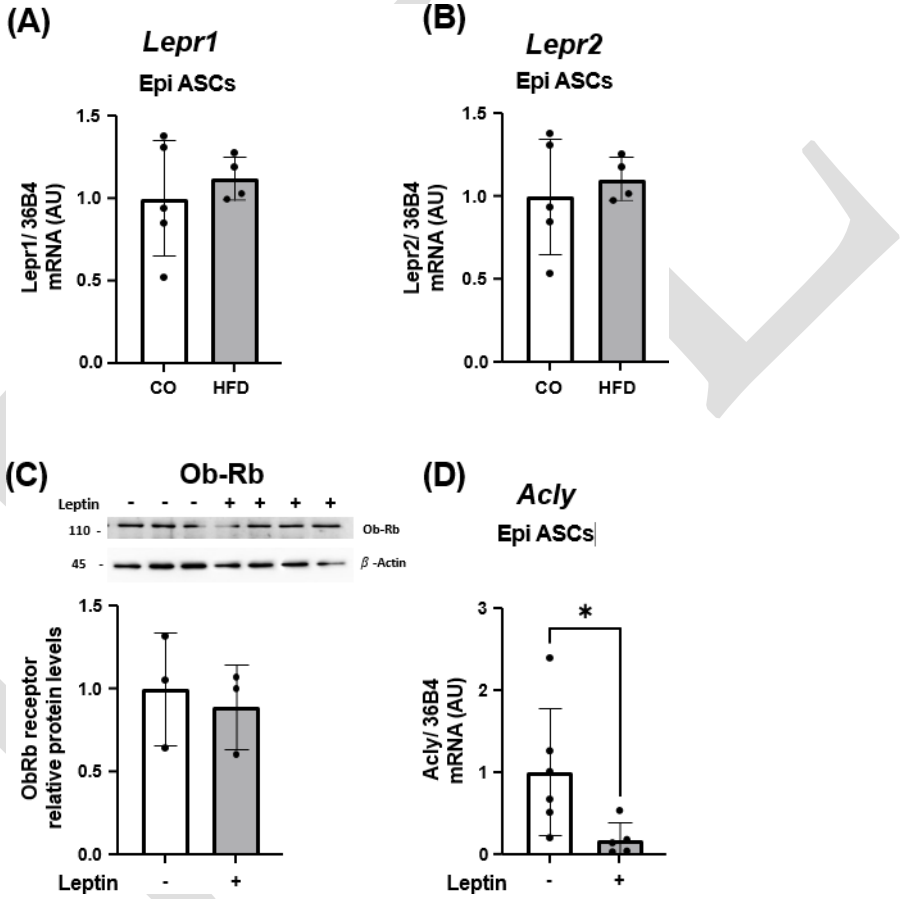

Figure 6. Gene expression of *Lepr1* (**A**) and *Lepr2* (**B**) in ASC isolated from WAT of animals that received a control diet (CO) or a high-fat diet (HFD). Total content of LEP R1 (Ob-Rb) protein (**C**) and gene expression of *Acly* (**D**) in ASC isolated from WAT of HFD-induced obese animals, treated in vitro with 100ng/mL leptin for 24 h. Data were analyzed using Student's *t*-test, and show mean ± SEM (n = 4–6). In (**A–C**), target genes were normalized by the constitutive *36B4*. In C, total content of protein was quantified by *ImageJ* and expressed in relation to the control and corrected by the expression of the constitutive beta-actin and total protein by Ponceau. A representative image of protein expression level is shown above the graphic. * $p < 0.05$.

2. Discussion

We looked at whether FO therapy, which is high in EPA, defends against the inflammatory pathway set off by HFD-induced obesity in WAT mice. Changes in the expression of several key genes involved in WAT metabolism and cell differentiation are connected with the activation of this pathway. Furthermore, we investigated if these effects are influenced by leptin (whose secretion is high in the WAT of obese people) and whether H3K27 changes mediate them. Based on our findings, FO may help reduce the harmful consequences of

obesity-related chronic inflammation via epigenetic pathways that affect ACL expression and H3K27 acetylation. In addition to being an essential endocrine signal, this work highlights leptin's paracrine involvement in influencing ASCs, which may influence their adipogenic capacity.

Mice that were given a high-fat diet for 16 weeks showed many changes, including an increase in visceral fat depot mass and an upregulation of genes that code for cytokines, macrophage chemotactic factors, macrophage markers, and inflammatory pathways. These results are consistent with what is already known about the many negative and severe consequences of the HFD [1]. Additionally, we found that a large number of genes that code for adiponectin, lipid biosynthesis enzymes, adipocyte receptors, pro- and anti-inflammatory cytokines, insulin signaling pathway components, browning, thermogenesis, and fatty acid oxidation are all part of the human genome. As a result of the HFD, the expression of 41 genes was found to be lowered. Interestingly, the long list of genes adversely impacted by the HFD was averted when the mice were treated with omega-3 polyunsaturated fatty acids (FO). In addition, the FO treatment up-regulated 32 genes, which aligned the results from these animals with the CO group and clearly separated them from the fat mice. All things considered, our findings show that FO therapy significantly affects the inflammatory pathway in WAT derived from HFD-treated mice via chemokine and cytokine signaling.

Additionally, the variety of changed genes was interesting overall, but the reversal of leptin expression after FO therapy really piqued our interest. When people are overweight and have chronic inflammation, their levels of the cytokine leptin, which controls how much energy adipocytes use, are much higher than normal. The results showed that leptin expression was 25 times higher in the HFD group as compared to the control group. Surprisingly, FO therapy did more than only turn back the clock; it also brought the visceral Epi WAT leptin expression levels down to levels lower than the control group. Hepatocytes and adipocytes exhibited decreased ACL enzyme expression in response to leptin [35]. Our results are supported by animal models of HFD-induced obesity, which usually show lower ACL expression in both hepatocytes and adipocytes [34-36]. The physiological effect of a high-fat diet (HFD) is to lower ACL expression and activity by reducing the need for new lipid synthesis, but the excess of dietary lipids from exogenous sources may keep esterification of fatty acids to triglycerides at a high level. Histone acetyltransferases [33] such as CREBBP and EP300 enhance H3K27 acetylation and ACL produces acetyl-CoA as a byproduct. This association establishes a link between its metabolism and the acetylation of proteins. Therefore, it is possible that there is less substrate available for histone acetylation due to a drop in cellular acetyl-CoA levels, as shown by the lower expression of Acly and ACL. This finding is in agreement with a previous research [34] and suggests that it probably happened in our model as well. Additionally, ACL is known to regulate gene expression via its effects on histone acetylation [31,38,40].

In this study, we found that in obese rats, there was an increase in leptin expression concomitant with a reduction in global H3K27ac levels and a coordinated down-regulation of Acly/ACL in the visceral WAT. Our findings point to a possible relationship between the decrease in ACL caused by HFD and the downregulation of substrate availability for the acetylase enzymes Ep300 and Crebbp. These enzymes' mRNA were probably up-regulated through a regulatory feedback system, which in turn led to the observed decrease in H3K27ac. Because H3K27ac is so important for transcriptional activation and chromatin accessibility, this decrease may have an effect on the many genes that are adversely impacted by the HFD.

Notably, FO therapy successfully counteracted the major up-regulation of leptin expression and the down-regulation seen in ACL and H3K27ac. The results of our current array study and earlier research [31] suggest that this H3K27ac reversal may help restore the control of genes that are often silenced in obesity. FO treatment not only protected the long list of genes

negatively impacted by the HFD (a total of 41 genes), but it also increased the expression of 32 genes, bringing the animals' expression profile closer to the control group and distinguishing them from the obese mice. Notably, FO entirely restored H3K27ac levels, demonstrating its ability to counteract obesity-related epigenetic alterations and providing evidence of a protective effect against the negative effects of HFD-induced obesity on gene expression patterns. If histone acetylation levels in WAT are affected by an HFD consumption, and if this impact is reduced by

Our results imply that with FO therapy, it may be possible to modify gene expression pathways associated with inflammation and adipogenesis.
Consistent with our results, several studies have shown that cancer cell lines and patients benefit from n-3 PUFA (EPA and DHA) diets, mostly due to the fact that these diets reduce inflammation via epigenetic processes [41,42]. Hyperacetylation of histones at some loci and N-terminal sections occurs worldwide as a consequence of this [43]. Histone acetylation is enhanced by an increase in free acetyl-CoA, which is caused by the inhibition of the enzyme ACC (Acetyl-CoA Carboxylase) in n-3 PUFA-rich diets [34,44]. Dietary changes also affect microRNA expression levels, most likely as a result of altered chromatin accessibility brought about by histone hyperacetylation [37].
The exact ways in which fish oil high in n-3 PUFA controls epigenetic marks in WAT, adipocytes, or ASCs are still unclear, however. It was difficult to separate the roles of adipocytes and ASCs since the studies presented here were carried out in WAT. While ASCs continue adipogenesis and develop into mature adipocytes to sustain renewal under "healthy" settings, WAT is significantly altered in "unhealthy" obesity [45]. The evidence points to dysregulated adipogenesis as the culprit disrupting WAT homeostasis in an obesogenic setting [46], with ASCs being pivotal in WAT remodeling during obesity [47].
Even while our understanding of the molecular pathways behind obesity is limited, we do know that epigenetic regulation is heavily involved in the years leading up to the disease's inception. Research shows that diminished adipogenic capacity and poor adipocyte maturation are caused by epigenetic dysfunction of ASCs, which is a major and possible regulatory event in obesity [48,49]. In addition, there is a dysfunctional pool of ASCs in WAT from people who are obese and/or have type 2 diabetes [50-53]. New research indicates that DNA methylation patterns are mostly maintained when cells commit to adipogenesis [48]. However, ASCs in obese people undergo a dynamic modification of DNA methylation in certain regions, which causes WAT dysfunction and metabolic syndromes. Environmental variables that promote obesity in the ASC niche have a significant impact on these epigenetic alterations. Although these studies have shown that ASCs play a key part in the process, little is known about how ASCs undergo epigenetic modifications in response to agents that might modulate them, whether in a healthy or diseased state.
We were motivated to delve more into the ASCs specialty by our discoveries in the overall WAT. Animals in the CO and HFD groups had their ASCs removed. The impact of leptin on ASC proliferation and differentiation has been highlighted in previous research [29,54,55]. When it comes to WAT from HFD obese mice, ASCs live in a constantly leptin-rich environment. They're supposed to attach to leptin receptors and use paracrine signaling to do their magic. Our research has shown that ASCs express the leptin receptor in two different isoforms: Lepr1 and Lepr2. Curiously, ASCs from obese mice showed no changes in the expression of Ob-Rb, the long isoform of the leptin receptor, when treated with in vitro leptin. This indicates that receptor expression remains constant even in the presence of obesity.
Then, we looked at how leptin affected Acly expression in ASCs. We have recently shown that, as in WAT, Acly is adversely regulated by an HFD and is substantially expressed in ASCs [56]. Acly silencing hinders histone acetylation and expression of certain genes, and one research shows that ACL connects cellular metabolism to histone acetylation during 3T3-L1 adipocyte development [31]. Unexpectedly, we found that ASCs grown with leptin had much lower levels of Acly expression. Consistent with previous research in obese WAT,

our results show that ASCs down-regulated Acly after prolonged exposure to a leptin-rich environment. These results provide new evidence that leptin signaling modulates ASC gene expression patterns and provide a possible mechanism by which obesity affects WAT functioning. We may learn more about the pathophysiology of obesity-related dysfunction in WAT if we dig further into the exact processes by which H3K27 acetylation and H3K27 methylation separate ASCs from adipocytes and macrophages. In an ongoing investigation, we are currently expanding upon this research.

In conclusion, during a 16-week research that aimed to cause obesity in mice by means of a high-fat diet (HFD), the diet increased the expression of genes linked to inflammation and macrophage markers while decreasing the expression of genes linked to adipokines, lipid biosynthesis, adipogenesis, and thermogenesis. The expression of H3K27 enzyme modifiers, as well as overall acetylation and methylation of H3K27, changed, according to epigenetic study. Folate supplementation throughout the final eight weeks somewhat mitigated these effects, indicating that it may have preventive benefits against obesity caused by the high-fat diet (HFD). Supporting a function in maintaining histone modifications, FO likewise averted decreases in ACL expression in obese animals. Taking FO supplements may help reduce the effects of the HFD on weight gain by affecting certain molecular and epigenetic mechanisms. To fully comprehend the impact of FO on H3K27 epigenetic markers, more study is required. Taken together, our results demonstrate that FO supplementation has a complex effect on adipose tissue's metabolic and epigenetic pathways, suggesting that it may be useful as a treatment for obesity-related dysregulation.

3. Materials and Methods

3.1. Animals, Fish Oil Supplementation, and Experimental Procedure

Male C57BL/6 mice, eight weeks old, were procured from CEDEME, which is part of UNFESP, the Federal University of São Paulo. Their living conditions were carefully regulated, including a 12-hour light-dark cycle and a constant temperature of 24 ± 1 °C. Eight weeks into the sixteen-week trial, the mice were split into two groups: six control (CO) mice with 9% fat, 76% carbohydrates, and 15% proteins, and twelve high-fat diet (HFD) mice with 26% carbs, 59% fat, and 15% proteins. For the second set of eight weeks, six animals were assigned to the HFD group that had already been separated into two subgroups: HFD alone and HFD + FO (fish oil supplementation). Fish oil supplementation was given orally three times weekly at a dose of 2 g/kg body weight. The supplement was supplied from HiOmega-3 (5:1 EPA/DHA, Naturalis Nutrição and Farma Ltd.a, São Paulo, Brazil). Our prior research [14,17] informed the selection of the FO dose and the 8-week treatment period; in those trials, the CO and HF groups also received water via gavage. Over the course of the 16 weeks, participants' weight and food consumption were tracked weekly. Isoflurane anesthesia and cervical dislocation were used to euthanize the mice after a 6-hour fast. Occipital plexus piercing was used to collect blood samples. The fat depots located in the abdomen (Epi and Rp) and under the skin (Ing) were removed, measured, and processed according to the steps outlined below.

3.2. The Tolerance to Sugar Test

During the 12th week of the trial, glucose tolerance tests (GTTs) were administered. Mice were administered 2 g kg−1 BW of glucose intraperitoneally after a 6-hour fast. Glucose levels in the tail vein were monitored using a OneTouch® glucometer at 15, 30, 45, 60, and 90 minute intervals. Every animal had its area under the curve determined.

3.3. How to Isolate the WAT and SVF

Collagenase digestion was carried out after immersing the Epi depot in digestion buffer and finely mincing it, in accordance with previously reported methods [57]. To summarize, the minced samples were mixed with a digestive buffer solution that contained Dulbecco's modified Eagle's medium, collagenase II, and other ingredients. The mixture was incubated at 37°C with orbital agitation set at 150 rpm for about 45 minutes. Next, the mixture was passed through a nylon mesh filter (Corning, Oneonta, NY, USA) and spun at 400× g for 1 minute. This separated

the mixture into two parts: the first was the supernatant, which contained the mature adipocytes that had been isolated; the second was the remaining filtrate, which contained the stromal vascular fraction (SVF). This filtrate was then spun at 1500× g for 10 minutes to create a cellular pellet. Following two washes, the pellet was aspirated. After that, the SVF was placed in an ice bath for 10 minutes with a

using a red blood cell lysis buffer (Manheim, Germany: Roche Diagnostics GmbH), followed by a wash with PBS and another round of centrifugation.

Treatment with leptin and isolation of ASCs (3.4)

We adhered to the steps outlined in the earlier description [56]. Basically, the cellular pellet (SVF) that was collected was mixed with culture medium (D'MEM Han's F-12, supplemented with 10% fetal bovine serum (FBS) and 10 mL/L penicillin/streptomycin; supplied by Gibco BRL, Oneonta, NY, USA)). The resulting suspension was then spread out in 100 mm culture dishes. These dishes were then placed in a 5% CO2 incubator at 37 °C, with medium changes every two days, until the cells reached 70-80% confluence. The plates were then washed with PBS after the medium was aspirated. On the first pass (P1), the cells were removed, resuspended in the same culture medium, seeded onto fresh culture plates for growth, and continued to be cultured until they achieved 70–80% confluence once again. Choosing the adherent cell population in the SVF was the last stage in isolating ASCs. Replating the cells followed the determination of cell concentration using a Neubauer chamber (P2). To ensure that confluence did not surpass 80%, cells were seeded for studies between passages P2 and P5 at a density of 1×10^1 cells/well on 6-well plates with a diameter of 35 mm. Cells were collected for mRNA and protein extraction when their density reached 85-90%. This was done either before or after a 24-hour treatment with leptin dissolved in culture media at a concentration of 100 ng/mL (Sigma Chemical, St. Louis, MO, USA). We considered each combined cell to be a single sample.

section 3.5. RNA extraction and qRT-PCR

Using Trizol reagent (Invitrogen Life Technologies, Waltham, MA, USA), total RNA was extracted from the whole Epi adipose depot or ASCs. Thermo Scientific's NANODROP One microvolume UVVis Spectrophotometers were used to measure ratios at 260/280 and 260/230 nm, which were used to evaluate the quality of the RNA. Thermo Scientific's Superscript III cDNA kit was used for reverse transcription to cDNA. by the Rotor gene (Qiagen, Dusseldorf, Germany) and SYBR Green fluorescent dye, gene expression was evaluated by quantitative real-time polymerase chain reaction (PCR), as reported in a previous work [56,58]. The findings were presented as the ratio of target gene expression to housekeeping genes (Gapdh and 36b4), and real-time PCR data analysis was carried out using the 2ΔΔCt technique. Table 2 contains the specific primer sequences.

Table 2. Sense and antisense primer sequences used for qRT-PCR.

Gene	5′ Primer (5′-3′)-Sense	3′ Primer (5′-3′)-Antisense
Gapdh	AAATGGTGAAGGTCGGTGTG	TGAAGGGGTCGTTGATGG
Ep300 (p300)	GTTGCTATGGGAAACAGTTATGC	TGTAGTTTGAGGTTGGGAAGG
Ezh2	CAGGATGAAGCAGACAGAAGAGG	TCGGGTTGCATCCACCACAAA
Kdm6a	GCTGGAACAGCTGGAAAGTC	GAGTCAACTGTTGGCCCATT
Kdm6b	CCTATTATGCTCCTGGGACA	TACGGCTTCCTCACTGTCGT
Crebbp (Cbp)	GACCGCTTTGTTTATACCTGC	TCTTATGGGTGTGGCTCTTTG
Acly	TCCGTCAAACAGCACTTCC	ATTTGGCTTCTTGGAGGTG
36b4 (Rplp0)	TAAAGACTGGAGACAAGGTG	GTGTACTCAGTCTCCAC AGA
Lepr1	CAGAATGACGCAGGGCTGTA	GCTCAAATGTTTCAGGCTTTTGG
Lepr2	ATTAATGGTTTCACCAAAGATGCT	AAGATCTGTAAGTACTGTGGCAT

Gapdh, Glyceraldehyde-3-phosphate Dehydrogenase; *Ep300 (p300)*, E1A binding protein p300; *Ezh2*, Enhancer of zest 2 polycomb repressive complex 2 subunit; *Kdm6a*, Lysine (K)-specific demethylase 6A; *Kdm6b*, Lysine (K)-specific demethylase 6B; *Crebbp*, CREB binding protein; *Acly*,

ATP citrate ly- ase; *36b4 (Rplp0)*, ribossomal protein lateral stalk subunit P0; *Lepr1*, leptin receptor 1; *Lepr2*, Leptin receptor 2.

3.2. PCR Array Gene Expression Analysis

For PCR array gene expression analysis, RNA was isolated using an RNA extraction kit following the manufacturer's instructions, and the assay was conducted as previously described [59]. Briefly, cDNA and RT2 SYBR® Green qPCR Mastermix (Cat. No. 330529) were utilized on a Custom Mouse RT2 Profiler PCR Array (CLAM30774R; Qiagen) con- sisting of 84 genes. This array allowed us to assess the expression pattern of genes encod- ing pro/anti-adipogenic, pro/anti-lipogenic and lipolytic, pro/anti-browning, adipokines, receptors, and components of adipocyte transduction pathways (see Table 3). CT values were exported and uploaded to the manufacturer's data analysis web portal at http://www.qiagen.com/geneglobe. Samples were categorized into control and test groups, and CT values were normalized based on a manual selection of reference genes. Fold Change was calculated using the $2^{\Delta\Delta Ct}$ method via the data analysis web portal (and exported at GeneGlobe®, Qiagen).

Table 3. List of selected genes in Custom Mouse RT2 Profiler PCR Array.

Pathways	**Genes**
Adipokines	*Adipoq (Acrp30), Cfd (Adipisin), Lep (leptin), Retn(Resistin)*
Lipases and lipogenic enzymes	*Acaca (Acc1), Gpd1 (glycerol-3-phosphate dehydrogenase 1 (soluble), Lipe(HSL),Scd1 (stearoyl CoA desaturase), Lpl, Pnpla2 (Atgl), Lipin 1, Pck1 (phosphoenolpyruvate carboxykinase 1), Fasn*
Pro-adipogenesis	*Cebpa, Cebpb, Cebpd, Pparg (PPAR gamma 2), Srebf1, Fabp4(aP2), Pilin1, Fgf2 (bFGF), Fgf10, Jun (c-jun ou AP1), Lmna (Lamini A), Sfrp1 (secreted frizzled-related protein1), Slc2a4 (Glut4), Klf15, Klf4*
Anti-adipogenesis	*Adrb2, Cdkn1a (p21Cip1, Waf1), Cdkn1b (p27Kip1), Ddit3 (Gadd153, Chop), Dlk1(Pref1), Foxo1, Ncor2, Shh, Sirt1, Wnt1, Wnt3a, Gata2, Klf*
Pro-Browning, fatty acid thermogenesis, and oxidation	*Bmp7, Cidea, Cpt1b, Creb1, Dio2, Elovl3, Foxc2, Mapk14 (p38alpha), Nrf1, Ppara, Ppard, Ppargc1a (Pgc1alpha), Ppargc1b (Perc, Pgc1beta), Prdm16, Sirt3, Src, Tbx1, Tfam, Ucp1, Wnt5a*
Anti-Browning	*Ncoa2, Nr1h3, Rb1, Wnt10b*
Adipokines receptors	*Lepr, Adipor2, Adrb1*
	Ccl2 (MCP1), Cxcl10, Ifng, Il1b, Il4, Il6, Il10, Il12b, Il13, Tgfb1, Tnf, Insr, Irs1, Irs2, Akt2,

Cytokines, growth factors,
and signal transduction *Ptpn1 (PTP1B), Ikbkb (IKKbeta), Mapk8 (JNK1), Nfkb1, Pik3r1 (p85alpha), Irf4, Retnla (Resistin-like alpha, Fizz1), Cd68*

Acaca (Acc1) provides the alpha-acetyl-Coenzyme A carboxylase. “Actin, beta” or “Actb” Akt2 is the thymoma viral proto-oncogene 2, Adipoq is adiponectin, Adipor2 is adiponectin receptor 2, Adrb1 is an adrenergic receptor beta 1, and Adrb2 is an adrenergic receptor beta 2. "B2m" stands for beta-2 microglobulin, while "Bmp7" pertains to bone morphogenetic protein 7. Chemokine ligand 2 (Ccl2); CD68 protein; Protein 21 (Cdkn1a) is an inhibitor of cyclin-dependent kinase, and Cdnk1b is an inhibitor of cyclin-dependent kinase, and Alpha CCAAT/enhancer binding protein (C/EBP), also known as Cebpa or C/EBPα. Cebpb, also known as C/EBPβ, is the beta form of the CCAAT/enhancer binding protein (C/EBP), whereas Cebpd is the delta form of the same protein. Cfd stands for complement factor D, which is found in adipsin. Cidea is the cell death-inducing DNA fragmentation factor alpha subunit like effector A. Cpt1b is the muscle carnitine palmitoyltransferase. Creb1 is the CAMP responsive element binding protein 1. Cxcl10 is the chemokine (C-X-C motif) ligand 10. Ddit3 is the DNA-damage inducible transcript 3. Dio2 is the deiodinase, iodothyronine, type II. Dlk1 (Pref-1) is the Drosophila beta-like 1 homolog. Elovl3 encodes a protein that is similar to FEN1/Elo2, SUR4/Elo3, and yeast-like 3. Adipocyte fatty acid binding protein 4 (Fabp4) and fatty acid synthase (Fasn) are two related acronyms. Fractal growth factor 2 (Fgf2) and fibroblast growth factor 10 (Fgf10) Two examples of forkhead boxes are Foxc2 and Foxo1. Gluceraldehyde-3-phosphate dehydrogenase, or Gapdh for short; Gpd1, short for soluble glycerol-3-phosphate dehydrogenase, and Gata2, short for GATA binding protein 2, Interferon gamma (Ifng) Inhibitor of kappaB kinase beta, which goes by the acronym IKKbeta. This is a list of interleukin numbers: Il10, Il12b, Il13, Il1b, Il4, and Il6. Every number represents a different interleukin. Insulin receptor coded as Insr; Insulin receptor substrates 1 and 2 are referred to as Irs1 and Irs2, respectively, while the Jun oncogene is abbreviated as Jun. KruppELF15, Klf2 (lung), and Klf4 (gut) are all KrappEL-like factors. lep—leptin; lepr—receptor for leptin; Lamin A; Lipe (HSL)—Hormone-sensitive lipase;

Apt acronym for "lipoprotein lipase" and "lipin 1." Mitogen-activated protein kinase 8 (Jnk1) and Mitogen-activated protein kinase 14 (Mapk14) are two examples of such proteins. Here are the acronyms for two proteins involved in nuclear receptor activation and repression: Ncoa2 and Ncor2. This gene enhancer in B-cells is called Nfkb1 and it is located at p105. Third member of nuclear receptor subfamily 1, group H; Phosphoenolpyruvate carboxykinase 1, cytosolic; Nuclear respiratory factor 1 (Nrf1) Pik3r1 stands for Phosphatidylinositol 3-kinase, regulatory subunit, polypeptide 1 (p85 alpha), Plin1 for Perilipin 1, Ppara for Peroxisome proliferator activated receptor alpha, Ppard for Peroxisome proliferator activator receptor delta, Pparg or PPARγ for Peroxisome proliferator activated receptor gamma, Ppargc1a for Peroxisome proliferative activated receptor, gamma, coactivator 1 alpha, and Ppargc1b for Peroxisome proliferative activated receptor, gamma, coactivator 1 beta. Protein tyrosine phosphatase, non-receptor type 1 (Ptpn1), retinal ganglion 1 (Rb1), resistin (Retn) and resistin-like alpha (Retnla) are all members of the PR domain. Rhino Transcription Control (RTC); Synonyms for "Scd1," "Rous sarcoma oncogene," "Sfrp1," and "Shh" include "stearoyl-coenzyme A desaturase 1" and "Sonic hedgehog," respectively. Solute carrier family 2 (Glut4) is a member of the facilitated glucose transporter family. Sirt1 and Sirt3 are homologs of Sirtuin 1 and Sirtuin 3, respectively, while Slc2a4 is a member of the Sirtuin family. The abbreviations Srebf1, Tbx1, and Tfam stand for "transcription factor A, mitochondrial" and "sterol regulatory element binding transcription factor 1," respectively. Transforming growth factor, beta 1 (TgA1) and tumor necrosis factor (TNF) are such acronyms. Mitochondrial uncoupling protein 1 (Ucp1), which carries protons; Wnt1 and Wnt10b are wingless-related MMTV integration sites, Wnt3a and Wnt5a are wingless-related MMTV integration sites, and Wnt6a is wingless-related MMTV integration site 6.

Western blot analysis. Nitrocellulose membranes with a thickness of 0.2 µm were used to transfer proteins extracted from Epi WAT depots (whole tissues) or ASCs after they were resolved using 12% or 15% sodium dodecyl sulfate (SDS)-polyacrylamide gel electrophoresis (PAGE). The membranes were first blocked with 5% albumin for 2 hours at room temperature. Then, they were incubated at 4 °C overnight with primary antibodies (#ab4729, #sab5700166, #ab40793, #ab5593, anti-H3K27ac, anti-ACL, anti-Leptin Receptor, Abcam, Wal-thamm, MA, USA). Secondary horseradish peroxidase-conjugated anti-rabbit IgG antibodies (Cell Signaling®, Danvers, MA, USA—#7074) were incubated with membranes at room temperature for 1 hour after washing. The ECL Prime Western Blotting System, manufactured by Amersham Biosciences® in Amersham, UK, is an enhanced chemiluminescence detection kit that was used to see the protein blots. Beta-actin levels were measured using an endogenous standard (#4967L) from Cell Signaling® in Danvers, MA, USA. This study used Scion Image software, developed by Scion Corporation in Frederick, MD, USA, to assess protein quantification. After adjusting for the expression of constitutive beta-actin and total protein by Ponceau, all data were expressed relative to the levels of the control group.

3.4. Analyzing Statistics

The figures show the results of the data analysis, which included one-way ANOVA, Tukey's post-test for comparisons across groups, and Student's t-test. We express the findings as the mean plus or minus the standard error of the mean (SEM). Any differences with a p-value less than 0.05 were deemed significant. We used GraphPad Prism 9.1.2, developed and published by GraphPad Software Inc. of San Diego, CA, USA, to conduct our statistical study. Tables and analyses in databases like UniProt and Gene Ontology Analysis were part of the RT2 Profiler PCR Array Data Analysis Software version 3.5 (SABiosciences, Frederick, MD, USA) used to examine the PCR array data.

4. Conclusions

Our research shows that epigenetic changes, especially H3K27ac and H3K27me3, play a key role in obesity-related WAT dysfunctions. These alterations are likely induced by the inflammatory environment, which includes obesity-rich leptin in obesity. This, in turn, may interfere with adipogenesis and/or adipocyte maturation, alter gene expression patterns, and worsen the chronic inflammatory state in a positive feedback loop. Considering the paucity of research on the correlation between FO therapy and WAT epigenetics, findings discoveries point to the possible function of FO in regulating these epigenetic variables and provide a promising strategy for dealing with consequences associated with obesity. The ongoing inflammatory state in obesity, disease pathogenesis, and potential therapeutic targets can be better understood by delving further into the symbiotic relationship between inflammation and H3K27 epigenetic marks during adipogenesis. This can be achieved through future investigations.

Funding: This research was funded by grants received from CNPq and FAPESP (2019/13618-9; 2022/15127-5; 2019/26240-4).

Institutional Review Board Statement: All procedures were approved by the Ethics Committee on Animal Use of the Federal University of São Paulo (CEUA nº 8827141217).

Informed Consent Statement: Not applicable.

Data Availability Statement: Data are contained within the article.

Acknowledgments: We would like to thank Roberta D. C. da Cunha de Sá, who collaborated with the gavages and tissue collections from the animals.

Conflicts of Interest: The authors declare no conflicts of interest. The funders had no role in the design of this study; in the collection, analyses, or interpretation of data; in the writing of the man- uscript, or in the decision to publish the results.

References

1. Li, J.; Wu, H.; Liu, Y.; Yang, L. High fat diet induced obesity model using four strains of mice: Kunming, C57BL/6, BALB/c and ICR. *Exp. Anim.* **2020**, *69*, 326–335. https://doi.org/10.1538/expanim.19-0148.
2. Prasad, M.; Rajagopal, P.; Devarajan, N.; Veeraraghavan, V.P.; Palanisam, C.P.; Cui, B.; Patil, S.; Jayaraman, S. A comprehensive review on high-fat diet-induced diabetes mellitus: An epigenetic view. *J. Nutr. Biochem.* **2022**, *107*, 109037. https://doi.org/10.1016/j.jnutbio.2022.109037.
3. Li, X.; Ren, Y.; Chang, K.; Wu, W.; Griffiths, H.R.; Lu, S.; Gao, D. Adipose tissue macrophages as potential targets for obesity and metabolic diseases. *Front. Immunol.* **2023**, *14*, 1153915. https://doi.org/10.3389/fimmu.2023.1153915.
4. Hotamisligil, G.S. Inflammation, metaflammation and immunometabolic disorders. *Nature* **2017**, *542*, 177–185. https://doi.org/10.1038/NATURE21363.
5. Yang, Z.H.; Chen, F.Z.; Zhang, Y.X.; Ou, M.Y.; Tan, P.C.; Xu, X.W.; Li, Q.; Zhou, S.B. Therapeutic targeting of white adipose tissue metabolic dysfunction in obesity: Mechanisms and opportunities. *MedComm* **2024**, *5*, e560. https://doi.org/10.1002/mco2.560.
6. Gilani, A.; Stoll, L.; Homan, E.A.; Lo, J.C. Adipose Signals Regulating Distal Organ Health and Disease. *Diabetes* **2024**, *73*, 169–177. https://doi.org/10.2337/dbi23-0005.
7. Schleh, M.W.; Caslin, H.L.; Garcia, J.N.; Mashayekhi, M.; Srivastava, G.; Bradley, A.B.; Hasty, A.H. Metaflammation in obesity and its therapeutic targeting. *Sci. Transl. Med.* **2023**, *15*, eadf9382. https://doi.org/10.1126/scitranslmed.adf9382.
8. Hawash, M.; Al-Smadi, D.; Kumar, A.; Olech, B.; Dominiak, P.M.; Jaradat, N.; Antari, S.; Mohammed, S.; Nasasrh, A.;

Abualha- san, M.; et al. Characterization and Investigation of Novel Benzodioxol Derivatives as Antidiabetic Agents: An In Vitro and In Vivo Study in an Animal Model. *Biomolecules* **2023**, *13*, 1486. https://doi.org/10.3390/BIOM13101486.
9. Hawash, M.; Jaradat, N.; Salhi, N.A.; Shatreet, B.; Asbah, A.A.; Hawash, Y.H. Assessing the therapeutic potential and safety of traditional anti-obesity herbal blends in Palestine. *Sci. Rep.* **2024**, *14*, 1919. https://doi.org/10.1038/S41598-024-52172-7.
10. Su, Y.; Choi, H.S.; Choi, J.H.; Kim, H.S.; Lee, G.Y.; Cho, H.W.; Choi, H.; Jang, Y.S.; Seo, J.W. Effects of Fish Oil, Lipid Mediators, Derived from Docosahexaenoic Acid, and Their Co-Treatment against Lipid Metabolism Dysfunction and Inflammation in HFD Mice and HepG2 Cells. *Nutrients* **2023**, *15*, 427. https://doi.org/10.3390/NU15020427.
11. Kapoor, B.; Kapoor, D.; Gautam, S.; Singh, R.; Bhardwaj, S. Dietary Polyunsaturated Fatty Acids (PUFAs): Uses and Potential Health Benefits. *Curr. Nutr. Rep.* **2021**, *10*, 232–242. https://doi.org/10.1007/S13668-021-00363-3.
12. Yu, S.; Xie, Q.; Tan, W.; Hu, M.; Xu, G.; Zhang, X.; Xie, G.; Mao, L. Different ratios of DHA/EPA reverses insulin resistance by improving adipocyte dysfunction and lipid disorders in HFD-induced IR mice. *Food Funct.* **2023**, *14*, 1179–1197. https://doi.org/10.1039/D2FO02686D.
13. Shahidi, F.; Ambigaipalan, P. Omega-3 Polyunsaturated Fatty Acids and Their Health Benefits. *Annu. Rev. Food Sci. Technol.* **2018**, *9*, 345–381. https://doi.org/10.1146/annurev-food-111317-095850.
14. de Sá, R.D.C.d.C.; Crisma, A.R.; Cruz, M.M.; Martins, A.R.; Masi, L.N.; do Amaral, C.L.; Curi, R.; Alonso-Vale, M.I. Fish oil prevents changes induced by a high-fat diet on metabolism and adipokine secretion in mice subcutaneous and visceral adipo- cytes. *J. Physiol.* **2016**, *594*, 6301–6317. https://doi.org/10.1113/JP272541.
15. de Sá, R.D.C.C.; Cruz, M.M.; de Farias, T.M.; da Silva, V.S.; de Jesus Simão, J.; Telles, M.M.; Alonso-Vale, M.I.C. Fish oil reverses metabolic syndrome, adipocyte dysfunction, and altered adipokines secretion triggered by high-fat diet-induced obesity. *Phys- iol. Rep.* **2020**, *8*, e14380. https://doi.org/10.14814/phy2.14380.
16. Antraco, V.J.; Hirata, B.K.S.; de Jesus Simão, J.; Cruz, M.M.; da Silva, V.S.; da Cunha de Sá, R.D.C.; Abdala, F.M.; Armelin-Correa, L.; Alonso-Vale, M.I.C. Omega-3 Polyunsaturated Fatty Acids Prevent Nonalcoholic Steatohepatitis (NASH) and Stim- ulate Adipogenesis. *Nutrients* **2021**, *13*, 622. https://doi.org/10.3390/nu13020622.
17. da Cunha de Sá, R.D.C.; Simão, J.d.J.; Silva, V.S.d.; Farias, T.M.d.; Cruz, M.M.; Antraco, V.J.; Armelin-Correa, L.; Alonso-Vale, M.I. Fish Oil Enriched in EPA, but Not in DHA, Reverses the Metabolic Syndrome and Adipocyte Dysfunction Induced by a High-Fat Diet. *Nutrients* **2021**, *13*, 754. https://doi.org/10.3390/nu13030754.
18. Iacobini, C.; Vitale, M.; Haxhi, J.; Menini, S.; Pugliese, G. Impaired Remodeling of White Adipose Tissue in Obesity and Aging: From Defective Adipogenesis to Adipose Organ Dysfunction. *Cells* **2024**, *13*, 763. https://doi.org/10.3390/cells13090763.
19. Johnston, E.K.; Abbott, R.D. Adipose Tissue Development Relies on Coordinated Extracellular Matrix Remodeling, Angiogen- esis, and Adipogenesis. *Biomedicines* **2022**, *10*, 2227. https://doi.org/10.3390/biomedicines10092227.
20. Mikkelsen, T.S.; Xu, Z.; Zhang, X.; Wang, L.; Gimble, J.M.; Lander, E.S.; Rosen, E.D. Comparative Epigenomic Analysis of Mu- rine and Human Adipogenesis. *Cell* **2010**, *143*, 156–169. https://doi.org/10.1016/j.cell.2010.09.006.
21. Zhao, Y.; Skovgaard, Z.; Wang, Q. Regulation of adipogenesis by histone methyltransferases. *Differentiation* **2024**, *136*, 100746. https://doi.org/10.1016/j.diff.2024.100746.
22. Jang, S.; Hwang, J.; Jeong, H.-S. The Role of Histone Acetylation in Mesenchymal Stem Cell Differentiation. *Chonnam Med. J.* **2022**, *58*, 6. https://doi.org/10.4068/cmj.2022.58.1.6.
23. Wei, Y.; Chen, Y.H.; Li, L.Y.; Lang, J.; Yeh, S.P.; Shi, B.; Yang, C.C.; Yang, J.Y.; Lin, C.Y.; Lai, C.C.; et al. CDK1-dependent phos- phorylation of EZH2 suppresses methylation of H3K27 and promotes osteogenic differentiation of human mesenchymal stem cells. *Nat. Cell Biol.* **2011**, *13*, 87–94. https://doi.org/10.1038/ncb2139.
24. Hemming, S.; Cakouros, D.; Isenmann, S.; Cooper, L.; Menicanin, D.; Zannettino, A.; Gronthos, S. *EZH2* and *KDM6A* Act as an Epigenetic Switch to Regulate Mesenchymal Stem Cell Lineage Specification. *Stem Cells* **2014**, *32*, 802–815. https://doi.org/10.1002/stem.1573.
25. Ogryzko, V.V.; Schiltz, R.L.; Russanova, V.; Howard, B.H.; Nakatani, Y. The Transcriptional Coactivators p300 and CBP Are Histone Acetyltransferases. *Cell* **1996**, *87*, 953–959. https://doi.org/10.1016/S0092-8674(00)82001-2.
26. Martins, V.F.; LaBarge, S.A.; Stanley, A.; Svensson, K.; Hung, C.W.; Keinan, O.; Ciaraldi, T.P.; Banoian, D.; Park, J.E.; Ha, C.; et al. p300 or CBP is required for insulin-stimulated glucose uptake in skeletal muscle and adipocytes. *JCI Insight* **2022**, *7*, e141344. https://doi.org/10.1172/jci.insight.141344. PMID: 34813504; PMCID: PMC8765050.
27. Akhter, N.; Kochumon, S.; Hasan, A.; Wilson, A.; Nizam, R.; Al Madhoun, A.; Al-Rashed, F.; Arefanian, H.; Alzaid, F.; Sindhu, S.; et al. IFN-γ and LPS Induce Synergistic Expression of CCL2 in Monocytic Cells via H3K27 Acetylation. *J. Inflamm. Res.* **2022**, *15*, 4291–4302. https://doi.org/10.2147/JIR.S368352.
28. Schuldt, L.; Reimann, M.; von Brandenstein, K.; Steinmetz, J.; Döding, A.; Schulze-Späte, U.; Jacobs, C.; Symmank, J. Palmitate- Triggered COX2/PGE2-Related Hyperinflammation in Dual-Stressed PdL Fibroblasts Is Mediated by Repressive H3K27 Tri- methylation. *Cells* **2022**, *11*, 955. https://doi.org/10.3390/cells11060955.
29. Takahashi, H.; McCaffery, J.M.; Irizarry, R.A.; Boeke, J.D. Nucleocytosolic acetyl-coenzyme a synthetase is required for histone acetylation and global transcription. *Mol. Cell* **2006**, *23*, 207–217. https://doi.org/10.1016/J.MOLCEL.2006.05.040.
30. Cluntun, A.A.; Huang, H.; Dai, L.; Liu, X.; Zhao, Y.; Locasale, J.W. The rate of glycolysis quantitatively mediates specific histone acetylation sites. *Cancer Metab.* **2015**, *3*, 10. https://doi.org/10.1186/S40170-015-0135-3.
31. Wellen, K.E.; Hatzivassiliou, G.; Sachdeva, U.M.; Bui, T.V.; Cross, J.R.; Thompson, C.B. ATP-citrate lyase links cellular metabo- lism to histone acetylation. *Science* **2009**, *324*, 1076–1080. https://doi.org/10.1126/SCIENCE.1164097.
32. Evertts, A.G.; Zee, B.M.; Dimaggio, P.A.; Gonzales-Cope, M.; Coller, H.A.; Garcia, B.A. Quantitative dynamics of the link be- tween cellular metabolism and histone acetylation. *J. Biol. Chem.* **2013**, *288*, 12142–12151. https://doi.org/10.1074/JBC.M112.428318.

33. Galdieri, L.; Zhang, T.; Rogerson, D.; Lleshi, R.; Vancura, A. Protein acetylation and acetyl coenzyme a metabolism in budding yeast. *Eukaryot. Cell* **2014**, *13*, 1472–1483. https://doi.org/10.1128/EC.00189-14.
34. Carrer, A.; Parris, J.L.D.; Trefely, S.; Henry, R.A.; Montgomery, D.C.; Torres, A.; Viola, J.M.; Kuo, Y.M.; Blair, I.A.; Meier, J.L.; et al. Impact of a High-fat Diet on Tissue Acyl-CoA and Histone Acetylation Levels. *J. Biol. Chem.* **2017**, *292*, 3312–3322. https://doi.org/10.1074/JBC.M116.750620.
35. Jiang, L.; Wang, Q.; Yu, Y.; Zhao, F.; Huang, P.; Zeng, R.; Qi, R.Z.; Li, W.; Liu, Y. Leptin contributes to the adaptive responses of mice to high-fat diet intake through suppressing the lipogenic pathway. *PLoS ONE* **2009**, *4*, e6884. https://doi.org/10.1371/JOURNAL.PONE.0006884.
36. Jin, H.; Kim, T.J.; Choi, J.H.; Kim, M.J.; Cho, Y.N.; Nam, K.I.; Kee, S.J.; Moon, J.B.; Choi, S.Y.; Park, D.J.; et al. MicroRNA-155 as
a proinflammatory regulator via SHIP-1 down-regulation in acute gouty arthritis. *Arthritis Res. Ther.* **2014**, *16*, R88. https://doi.org/10.1186/ar4531.
37. Peng, M.; Yin, N.; Chhangawala, S.; Xu, K.; Leslie, C.S.; Li, M.O. Aerobic glycolysis promotes T helper 1 cell differentiation through an epigenetic mechanism. *Science* **2016**, *354*, 481–484. https://doi.org/10.1126/science.aaf6284.
38. Margueron, R.; Reinberg, D. The Polycomb complex PRC2 and its mark in life. *Nature* **2011**, *469*, 343–349. https://doi.org/10.1038/nature09784.
39. Lee, J.V.; Carrer, A.; Shah, S.; Snyder, N.W.; Wei, S.; Venneti, S.; Worth, A.J.; Yuan, Z.F.; Lim, H.W.; Liu, S.; et al. Akt-dependent metabolic reprogramming regulates tumor cell histone acetylation. *Cell Metab.* **2014**, *20*, 306–319. https://doi.org/10.1016/J.CMET.2014.06.004.
40. Amatruda, M.; Ippolito, G.; Vizzuso, S.; Vizzari, G.; Banderali, G.; Verduci, E. Epigenetic Effects of n-3 LCPUFAs: A Role in Pediatric Metabolic Syndrome. *Int. J. Mol. Sci.* **2019**, *20*, 2118. https://doi.org/10.3390/ijms20092118.
41. Georgel, P.T.; Georgel, P. Where Epigenetics Meets Food Intake: Their Interaction in the Development/Severity of Gout and Therapeutic Perspectives. *Front. Immunol.* **2021**, *12*, 752359. https://doi.org/10.3389/fimmu.2021.752359.
42. Abbas, A.; Witte, T.; Patterson, W.L., 3rd; Fahrmann, J.F.; Guo, K.; Hur, J.; Hardman, W.E.; Georgel, P.T. Epigenetic Reprogram- ming Mediated by Maternal Diet Rich in Omega-3 Fatty Acids Protects From Breast Cancer Development in F1 Offspring. *Front. Cell Dev. Biol.* **2021**, *9*, 682593. https://doi.org/10.3389/fcell.2021.682593.
43. Galdieri, L.; Vancura, A. Acetyl-CoA Carboxylase Regulates Global Histone Acetylation. *J. Biol. Chem.* **2012**, *287*, 23865–23876. https://doi.org/10.1074/jbc.M112.380519.
44. Yu, G.; Floyd, Z.E.; Wu, X.; Hebert, T.; Halvorsen, Y.D.; Buehrer, B.M.; Gimble, J.M. Adipogenic Differentiation of Adipose-Derived Stem Cells. In *Adipose-Derived Stem Cells. Methods in Molecular Biology*; Gimble, J., Bunnell, B., Eds.; Humana Press: Totowa, NJ, USA, 2011; Volume 702, pp. 193–200. https://doi.org/10.1007/978-1-61737-960-4_14.
45. Patel, P.; Abate, N. Role of Subcutaneous Adipose Tissue in the Pathogenesis of Insulin Resistance. *J. Obes.* **2013**, *2013*, 1–5.
https://doi.org/10.1155/2013/489187.
46. Cawthorn, W.P.; Scheller, E.L.; MacDougald, O.A. Adipose tissue stem cells meet preadipocyte commitment: Going back to the future. *J. Lipid Res.* **2012**, *53*, 227–246. https://doi.org/10.1194/jlr.R021089.
47. Ejarque, M.; Ceperuelo-Mallafré, V.; Serena, C.; Maymo-Masip, E.; Duran, X.; Díaz-Ramos, A.; Millan-Scheiding, M.; Núñez-Álvarez, Y.; Núñez-Roa, C.; Gama, P.; et al. Adipose tissue mitochondrial dysfunction in human obesity is linked to a specific DNA methylation signature in adipose-derived stem cells. *Int. J. Obes.* **2019**, *43*, 1256–1268. https://doi.org/10.1038/s41366-018- 0219-6.
48. Pérez, L.M.; Bernal, A.; de Lucas, B.; San Martin, N.; Mastrangelo, A.; García, A.; Barbas, C.; Gálvez, B.G. Altered Metabolic and Stemness Capacity of Adipose Tissue-Derived Stem Cells from Obese Mouse and Human. *PLoS ONE* **2015**, *10*, e0123397. https://doi.org/10.1371/journal.pone.0123397.
49. Serena, C.; Keiran, N.; Ceperuelo-Mallafre, V.; Ejarque, M.; Fradera, R.; Roche, K.; Nuñez-Roa, C.; Vendrell, J.; Fernández-Veledo, S. Obesity and Type 2 Diabetes Alters the Immune Properties of Human Adipose Derived Stem Cells. *Stem Cells* **2016**, *34*, 2559–2573. https://doi.org/10.1002/stem.2429.
50. Pachón-Peña, G.; Serena, C.; Ejarque, M.; Petriz, J.; Duran, X.; Oliva-Olivera, W.; Simó, R.; Tinahones, F.J.; Fernández-Veledo, S.; Vendrell, J. Obesity Determines the Immunophenotypic Profile and Functional Characteristics of Human Mesenchymal Stem Cells From Adipose Tissue. *Stem Cells Transl. Med.* **2016**, *5*, 464–475. https://doi.org/10.5966/sctm.2015-0161.
51. Crujeiras, A.B.; Diaz-Lagares, A.; Moreno-Navarrete, J.M.; Sandoval, J.; Hervas, D.; Gomez, A.; Ricart, W.; Casanueva, F.F.; Esteller, M.; Fernandez-Real, J.M. Genome-wide DNA methylation pattern in visceral adipose tissue differentiates insulin-re- sistant from insulin-sensitive obese subjects. *Transl. Res.* **2016**, *178*, 13–24.e5. https://doi.org/10.1016/j.trsl.2016.07.002.
52. Roldan, M.; Macias-Gonzalez, M.; Garcia, R.; Tinahones, F.J.; Martin, M. Obesity short-circuits stemness gene network in human adipose multipotent stem cells. *FASEB J.* **2011**, *25*, 4111–4126. https://doi.org/10.1096/fj.10-171439.
53. Palhinha, L.; Liechocki, S.; Hottz, E.D.; Pereira, J.A.D.S.; de Almeida, C.J.; Moraes-Vieira, P.M.M.; Bozza, P.T.; Maya-Monteiro, C.M. Leptin Induces Proadipogenic and Proinflammatory Signaling in Adipocytes. *Front. Endocrinol.* **2019**, *10*, 487057. https://doi.org/10.3389/fendo.2019.00841.
54. Crop, M.J.; Baan, C.C.; Korevaar, S.S.; Ijzermans, J.N.M.; Weimar, W.; Hoogduijn, M.J. Human Adipose Tissue-Derived Mesen- chymal Stem Cells Induce Explosive T-Cell Proliferation. *Stem Cells Dev.* **2010**, *19*, 1843–1853. https://doi.org/10.1089/scd.2009.0368.
55. da Silva, V.S.; Simão, J.J.; Plata, V.; de Sousa, A.F.; da Cunha de Sá, R.D.C.; Machado, C.F.; Stumpp, T.; Alonso-Vale, M.I.C.; Armelin-Correa, L. High-fat diet decreases $H3K27_{ac}$ in mice adipose-derived stromal cells. *Obesity* **2022**, *30*, 1995–2004.

https://doi.org/10.1002/oby.23537.
56. Rodbell, M. Metabolism of isolated fat cells. I. Effects of hormones on glucose metabolism and lipolysis. *J. Biol. Chem.* **1964**, *239*, 375–380. PMID: 14169133.
57. Reeves, P.G.; Rossow, K.L.; Lindlauf, J. Development and Testing of the AIN-93 Purified Diets for Rodents: Results on Growth, Kidney Calcification and Bone Mineralization in Rats and Mice. *J. Nutr.* **1993**, *123*, 1923–1931. https://doi.org/10.1093/jn/123.11.1923.